Mekkawi et al., J Geol Geophys 2018, 7:1
DOI: 10.4172/2381-8719.1000318

Journal of Geology & Geophysics
ISSN: 2381-8719

Research Article Open Access

Three Dimensional Modelling of Kharga Reservoir Water, New Valley-Egypt, Using Magnetotelluric Data

Mahmoud Mohamed Mekkawi[1]*, Tarek Arafa-Hamed[1], Puwis Amatykul[2], Yasuo Ogawa[3] and Magdy Atya[1]

[1]*National Research Institute of Astronomy and Geophysics, 11722 Helwan, Egypt*
[2] *Geophysical Research Group, Faculty of Science, Mahidol Univ., Bankok 10400, Thailand*
[3]*Volcanic Fluid Research Center, Tokyo Institute of Technology, Tokyo 152-8551, Japan*

Abstract

Most of the Egyptian populations live along the two banks of the Nile River in order to access water for daily needs and other purposes. About 90% of Egyptian territories is a desert with little amount of rainfall. In these arid deserts, groundwater is the only possible source that would support cultivation and civil expansions. Several Oases including Kharga are distributed in the western desert of Egypt, in which the groundwater is the main source of irrigation and daily life. The New-Valley governorate is keen on reclaiming the western desert and developing new urban areas. Previously available boreholes and geological information are used to preliminary evaluate the three dimensional (3D) subsurface structures including the reservoir water and its environment.

In this study we utilize magnetotelluric (MT) recordings to spot more light on the Nubian aquifer of the Kharga Oasis. A 3D-MT inversion is applied using "w3dinvmt" code. The resultant 3D-resistivity indicates a low resistive layer associated with a Quaternary aquifer and extends from the surface down to a depth more than 50 m. Low to moderate resistivity values are found to indicate a deep Cretaceous aquifer defined at depths from 250 m to 500 m. A resistive zone is found to exist between them that can be associated with solidified limestone and phosphate layers. Furthermore, a high resistivity value appears to belong to the basement complex of Precambrian rocks in the Oasis. A constructed 3D-model is well matching with major hydro-geological structure of the Kharga Oasis that has been inferred from previous works.

Keywords: New Valley; Kharga Oasis; Reservoir Water; 3D Magnetotelluric Modeling

Introduction

Egypt suffers a continuous decreasing in water resources, resulting from constructing many dams on the river Nile as in Sudan and Ethiopia. The river extends in Egypt for more than 1000 km and is a main source of water required for life and agricultural purposes. The Kharga Oasis lies between latitudes 24º00` - 26 º00` N and longitudes 30° 00 - 31º 00 E. It represents a region of the new valley governorate which includes Siwa, Bahariya, Farafra, Dakhala and Baries Oases. It is considered as a depression (basin) and is characterized by surface springs, playa and sand dunes. The reservoir water extends for more than 125 km from north Kharga city to Baris Oasis in the south with a width of about 25 km, covering an area of 3125 km^2. It lies more than 200 km far from the River Nile (Figure 1). As groundwater is the only source for agricultural areas, the evaluation of reservoir waters needs more information about its spatial extents and depths as well as about the sources of recharging.

It is well known that MT is sensitive for electrically conductive layers. In this study an attempt to evaluate the environmental and regional structures of the reservoir water at Kharga Oasis using 3D-MT and compare the results with previously constructed models based on geological studies supported by borehole logs.

Hydro-geology and Boreholes Information

The geology of Kharga Oasis has been reported by several authors [1,2]. It is subjected, as well, to comprehensive studies of hydro-geology, geochemistry and geophysics by [3-6]. According to these works, the Kharga reservoir is divided into three main basins as: Kharga, north Kharga and south Kharga as based on aerial photography and wells information. The structures at these three zones lead to conclude that; 1) A main N-S fault extension draw the longer axis of Kharga main basin; 2) the E-W fault extensions control the width of the basins and the rechargeable water in the reservoir [7].

During a span of 40 years from 1967 to 2007, the groundwater level dropped from 60 m to 80 m below the ground in the northern part of Kharga Oasis, while dropped from 40 to 60 m in the southern part as shown in Figure 2, During the ten years (2003-2013), the number of deep well (Figure 3) increased to 350, and hence, the reservoir water level dropped for more than 90 m, due to the high consuming rate and over-exploitation of the groundwater (Dept. of water resources in Kharga, Personal Communication).To the south of Kharga City, natural springs of Bulaq and Nasser villages are famous for its water temperature reaching up to 45°C (Figure 3) and its effect for the treatment of rheumatism and allergies [1].

The upper horizons of reservoir are divided into two main aquifers which are the Quaternary and the Cretaceous ones. The two systems are different in thickness and lithology. The ground waters of the Quaternary aquifers are of shallow depths, from surface (0 m) down to 50 m and recharge directly from irrigation water. The Cretaceous aquifers are exists at a deeper range from 250 to 500 m with a transmissivity range

***Corresponding author:** Mahmoud Mohamed Mekkawi, Professor, Department of Applied Geophysics, National Research Institute of Astronomy and Geophysics, Egypt, Tel: +201000643221; +20233836327; E-mail: mekkawi05@yahoo.com

Received September 07, 2017; **Accepted** December 04, 2017; **Published** December 11, 2017

Citation: Mekkawi M, Arafa-Hamed T, Amatykul P, Atya M, Ogawa Y (2017) Three Dimensional Modelling of Kharga Reservoir Water, New Valley- Egypt, Using Magnetotelluric Data. J Geol Geophys 7: 318. doi: 10.4172/2381-8719.1000318

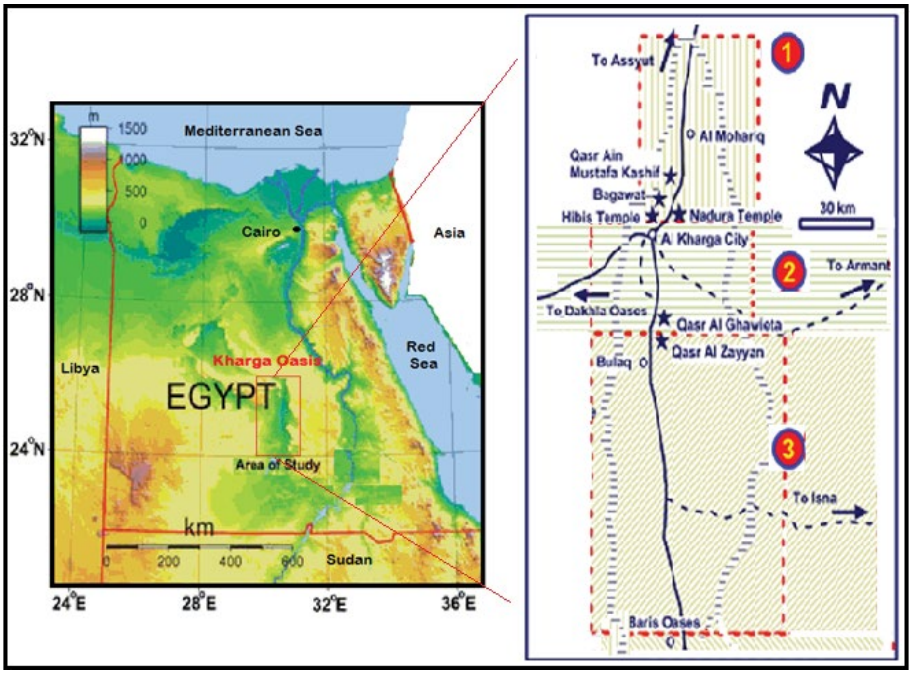

Figure 1: Location map of Kharga Oasis area and boundary of its Reservoir Water (Red dash line).

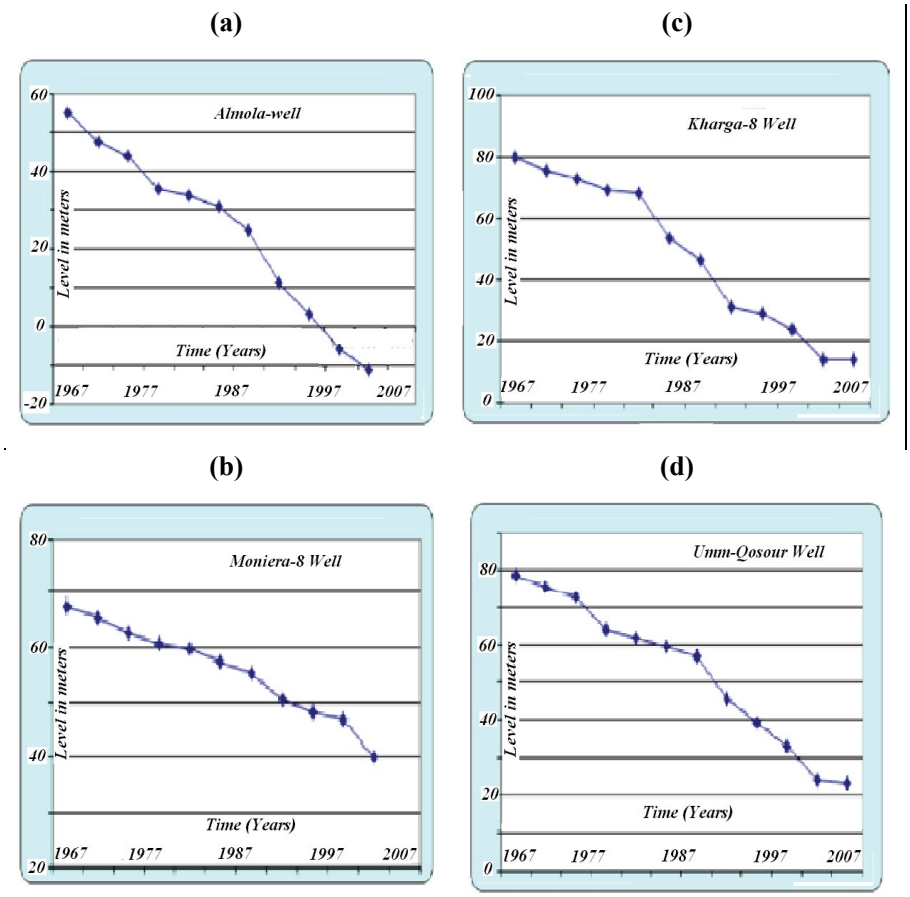

Figure 2: Observed drops of KRW level 60-80 m in the northern wells **(a)** Almola, **(b)** Moniere-8, **(c)** Kharga-8 and **(d)** Umm-Qosour, during the period 1967-2007 (Dept. of water resources in Kharga, personal communication).

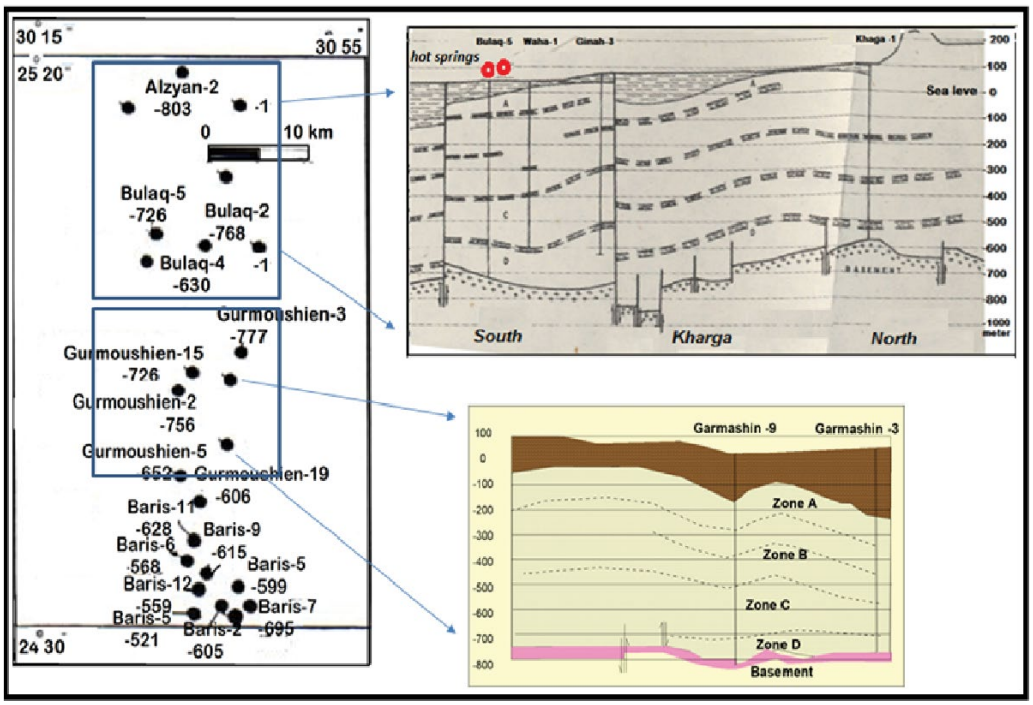

Figure 3: Location map of some boreholes reached to basement (**left**) and cross-sections from south to North showing the different horizons of water Reservoir (**right**).

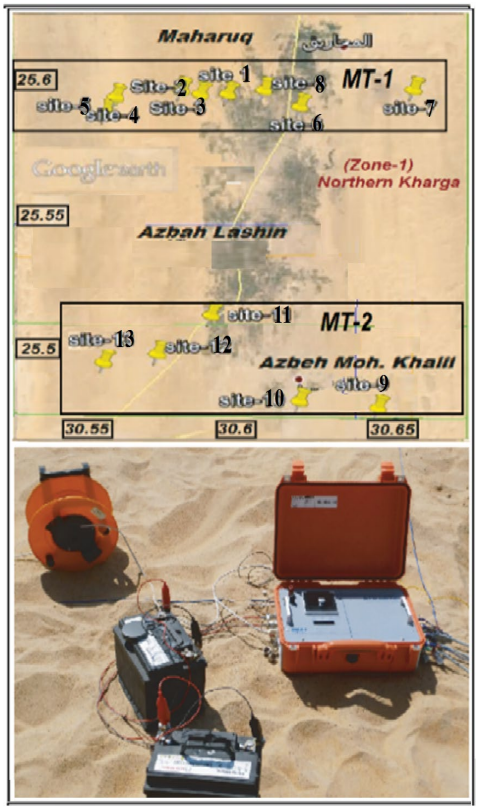

Figure 4: Location of two MT Profiles (**upper**) and broadband system (ADU-7e) used in Kharga Oasis area (**lower**).

from 350-600 m^3/day, which is suitable for irrigation and drinking purposes. The deeper wells have salinity range from 513 to 1444 ppm, while shallower wells and springs vary in salinity between 308 to 4078 ppm. The ground waters of deeper wells are costly expensive for drilling and energy consumption but recharge from the Nubian sandstone aquifers [1]. The saturated thicknesses of shallow and deep wells are different according to the water penetration rate [5].

Magnetotelluric Data

The MT method uses the Earth's natural occurring electromagnetic fields to investigate the electrical resistivity structure of the subsurface from shallow depths (tens of meters) to deep depths [8]. On the other hand, electrical resistivity of a lithology is dependent on the existence of fluids, clay minerals and porosity in the rocks. The MT data were collected using EDU-7e MT system [9] designed for broadband survey (0.001-1000 s), audio-magnetotelluric (AMT) and magnetotellric (MT). The MT system and acquisition in Kharga Oasis are illustrated in (Figure 4). The software for data processing is updated using (Procmt & Mapros) programs for processing [9]. The MT data is acquired during a field trip in two profiles in the northern part of the Kharga reservoir which consists of 13 stations after omitting noisy soundings (Table 1). The station separations are different in distance (1-3 km), due to the hard topography and sand dunes. The time series are edited manually to remove sections contaminated by cultural noise. The MT data quality appeared then to be of a good quality (Figure 5).

Preliminary images of electrical resistivity models (Figure 6) using Bostick, Occam [10] and Rebocc codes [11] are estimated [12]. The results are compared with the boreholes information and subsurface structures. Both 1D-MT models (Bostick & Occam) show the variations of vertical resistivity with depth (Figures 6 a and b), while the result of 2D-MT (Rebocc) is presented for several zones of distinctive resistivities

Site Name	Longitude	Latitude	Elevation	Remarks
1	30° 33' 30.97" E	25° 26'20.54" N	43.25 m.	
2	30° 37' 03.70" E	25° 35'58.14" N	42.80 m.	
3	30° 36' 44.93" E	25° 36'02.68" N	60.01 m.	
5	30° 35' 30.97" E	25° 35'37.35" N	58.61 m.	
6	30° 38' 40.72" E	25° 35'44.50" N	49.01 m.	
7	30° 40' 31.66" E	25° 36'02.82" N	70.01 m.	
8	30° 38' 05.82" E	25° 36' 02.68" N	54.45 m.	
9	30° 39' 57.0" E	25° 30' 8.6" N	57.1 m.	
10	30° 38' 40.4" E	25° 30 16.5" N	57.70 m.	
11	30° 37' 14.1" E	25° 30' 33.7" N	49.50 m.	
12	30° 36' 22.1" E	25° 31' 8.8" N	51.20 m.	
13	30° 35' 28.8" E	25° 30' 58.9" N	46.45 m.	

Table 1: MT sites

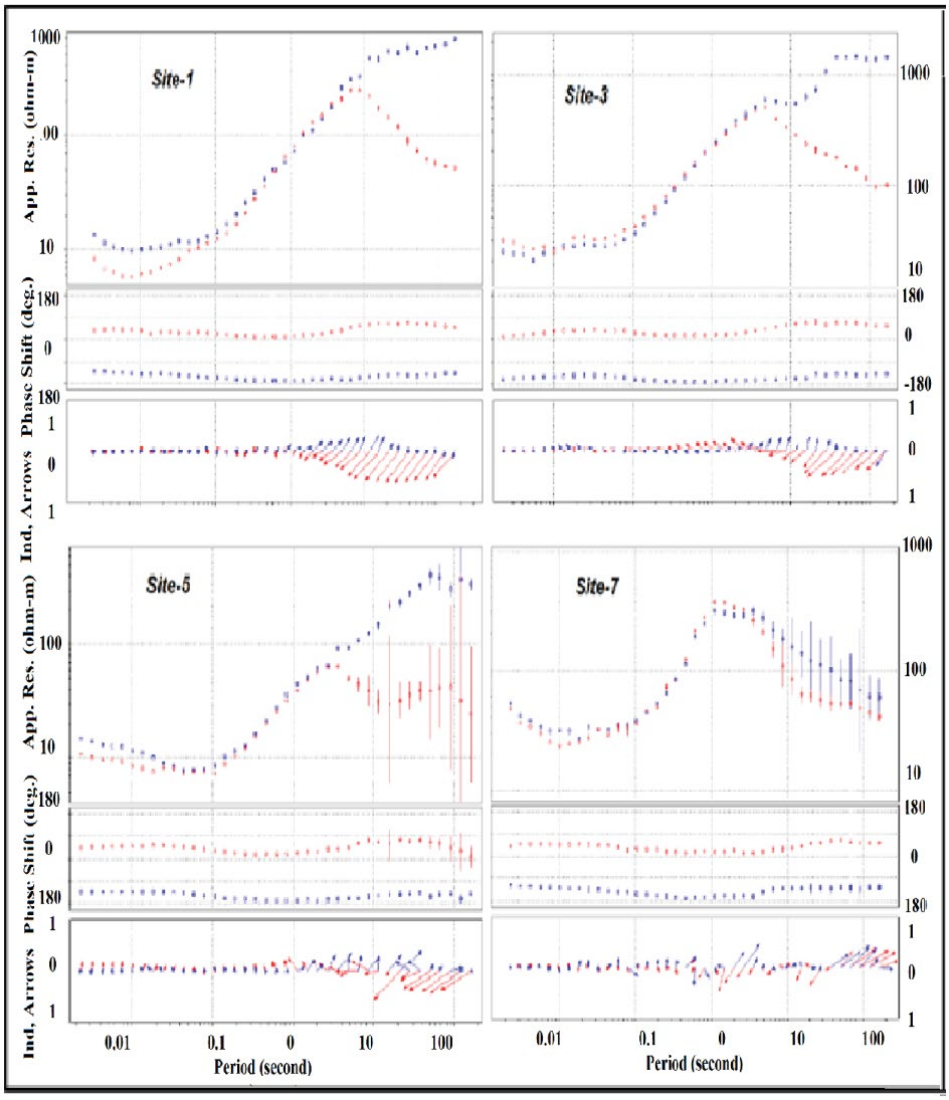

Figure 5: Example of MT Soundings stations, apparent resistivity & phase in two modes TE (red), TM (blue), and induction arrows in real (red) and imaginary (blue).

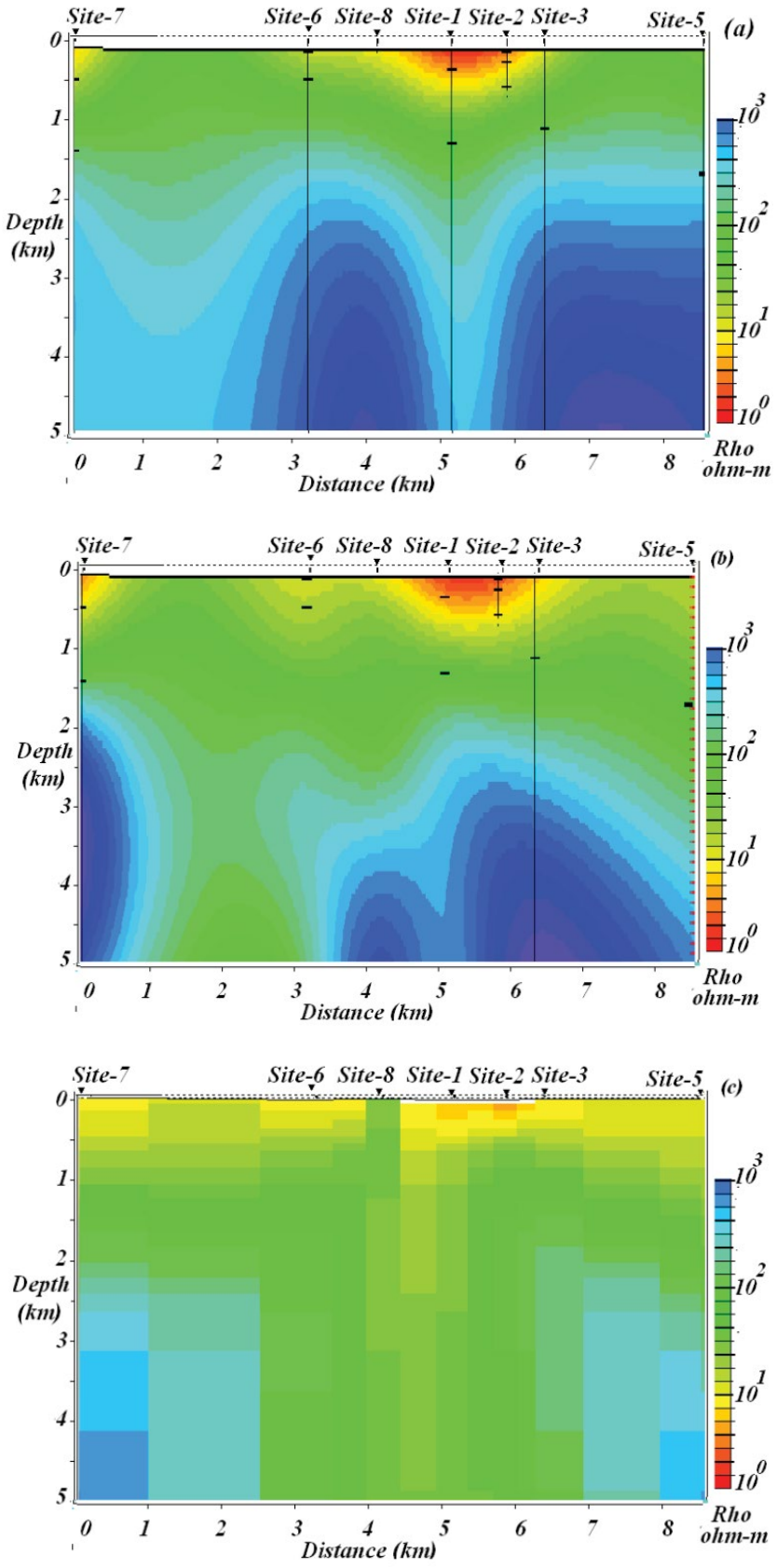

Figure 6: (a) 1D-MT models using Bostick (**upper**), (b) Occam (**middle**) and (c) 2D-MT model using Rebocc (**lower**), respectively.

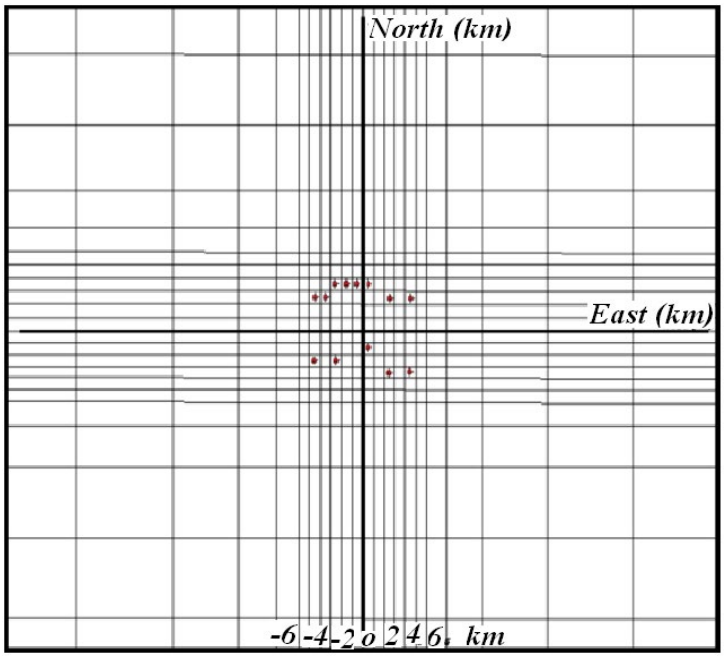

Figure 7: The mesh parameter 100 × 100 × 100 km, core cell width is 1 km and resistivity half space=100 ohm-m.

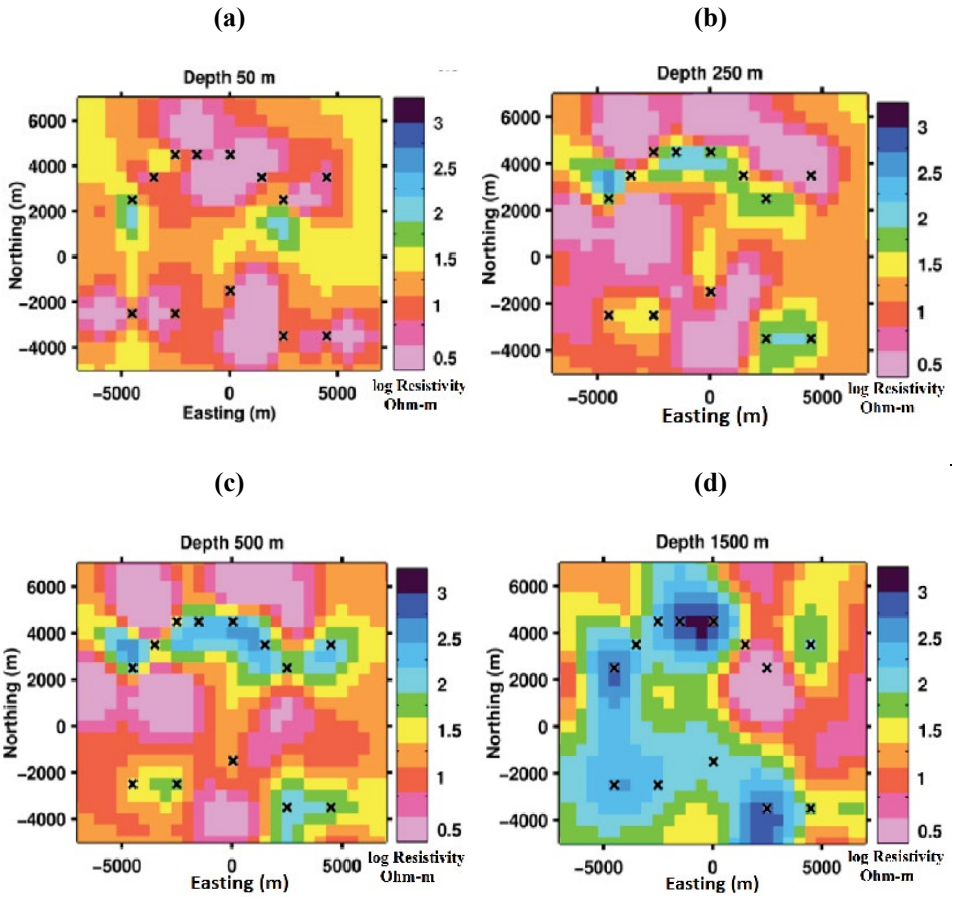

Figure 8: Horizontal slice through 3D resistivity model at different depths **(a)** 50 m, **(b)** 250 m, **(c)** 500 m and **(d)** 1500 m above sea level. **Black crosses** correspond to the location of MT stations.

(Figure 6c). In general, the resistivity increases with depth, except those of the near surface layers (low resistive) of Quaternary sediments and those with low to moderate resistivity of Cretaceous [12].

Three Dimensional modeling

The 3D-MT inversion modeling is applied using "wsinv3dmt" code provided by Siripunvarapurn [11]. The number of periods and responses should not exceed the parameter set in 'para.h' of the code. The number of periods are chosen 3 per decade, and 4 responses are supported to the off diagonal impedances (Zxy and Zyx) respectively. The 3D-MT forward and inverse modeling has been reported by many authors since 90's [13-22]. It has also been tested and developed with different data sets from land and marine environments [23-27].

The "wsinv3dmt" code is used not only for gridded data but also for data acquired along profiles [11,28]. They interpreted 2D-MT profile data using a 3D approach. The profiles can be put together or separately using a code for single processor machine. A 3D minimum structure inversion is based on a data-space variant of the Occam scheme [10, 28,29].

Generally speaking, a 3D inversion is associated with long time consumption and requires a large accessory memory. All computations are performed in this study using a UNIX system with 8 GB RAMS. The "wsinv3dmt" code forms the full Jacobian of the model parameter data mapping. The 13 periods selected for the inversion are from 0.01 sec. to 10 sec. The impedances are rotated to be consistent with the coordinate system which is oriented in cross-strike illustrating the orientation of (N-S) and (E-W).

The model grid dimensions are Nx=28, Ny=28 and NZ=23 (plus 7 air layers). The mesh is created with a vertical factor of 1.2 and with a top-layer thickness 100 m (Figure 7). The horizontal grid spacing is 1 km in the central part and increases in both side until total model domain spacing of 100 × 100 × 100 km. Data error is set for the inversion as 10 % root mean square of Zxy × Zyx.

The initial model is homogeneous half space where the resistivity is 100 ohm-m. The results of 3D inversion are obtained at 3 iterations. The normalized RMS misfit is 3.5 and took place after 120 hours. The 3D-resistivity horizontal slices of the reservoir model at different depths (50, 250, 500 and 1500 m) are shown in (Figure 8). Also, 3D- resistivity can describe in the vertical cross-sections slices with depths (Figure 9).

Results & Conclusion

The 3-D resistivity structures of the Kharga Oasis (Figures 8 & 9) are characterized as following

The conductive thin layer (Figure 8 a and b) has resistivity (10-100 ohm-m) extends to more than 50 m and represent shallow aquifer of Quaternary sediments. It can be rechargeable from water of irrigation

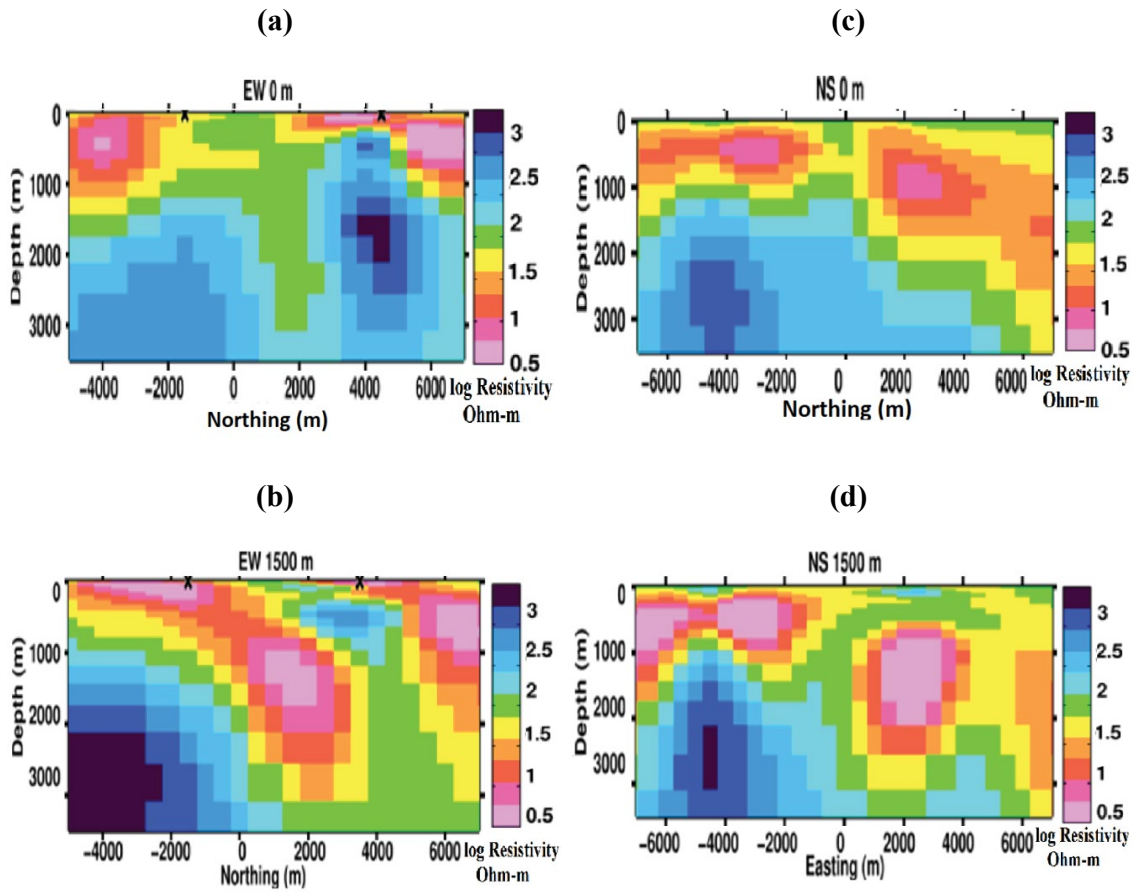

Figure 9: Vertical **c**ross-sections slice through 3D-resistivity model at different depths **(a)** E-W 0 m, **(b)** E-W 1500 m, **(c)** N-S 0 m and **(d)** N-S 1500 m above sea level. **Black crosses** correspond to the location of MT stations.

which contains some salts and fertilizers. Also, it can be interpreted as a zone of clay, plya and shale. This kind of aquifer can be used in agriculture only. Also, mixed limestone and phosphate layer (Paleocene rocks) at depth 50-250 serve as barrier between fresh and salinity water. Also, it is play a role of the cap-rock of the reservoir water system in the region.

-There are conductive layers of deep aquifer (Figure 8 b and c) belongs to cretaceous rocks and has thick layer of sediments (750 m) which starts 250 m and reachs to basement rock. The salinity range (300-1000 ppm) which is suitable for irrigation and daily life. The lithology consists of siltstone, sandstone with shale. The source of recharge is Nubian Sandstone Aquifer (NSA) which is the largest water aquifer systems (5 million cubic feet) of groundwater located in the eastern portion of the Sahara Desert [5].

-The conductive zones at depths 1500-2000m (Figures 9a, b, c and d) have resistivity between (50-100 ohm-m), could be the source of surface natural springs and geothermal activity in the area.

-The high resistive layers (blue color) are associate with and basement complex of Pre-Cambrian rocks.

The 3D resistivity model is reliable than previous 1D and 2D models and adds more detail information to the reservoir water of Kharga Oasis. The extension and change of resistivity with different depths are manifested.

Recommendation

It is recommended that to carry out more MT stations to cover the boundary of water reservoir and using different geophysical tools like seismic velocity analysis, gravity and magnetic methods.

Acknowledgement

Special thank is due to Prof. Magdy Atya, principle investigator (PI) of STDF Kharga project for financial support and providing the chance to carry out magnetotelluric survey in Kharga Oasis. At Tokyo Institute of Technology, Prof Yasuo Ogawa, gave me all support and encouragement during interpretation. Also many thanks to Dr. Puwis Amatykul, Mahidol Univ, Bankok-Thailand for helping me during research work.

References

1. Goubachi S, Baraka A (2006) Geological settings and their bearing upon the occurrences of shallow water bearing horizon in north kharga depression, western Desert, Egypt. Bull of Desert Research Center 1(1).
2. Klitzsch E, Hermina M (1989) The Mesozoic. In Stratigraphic lexicon and explanatory notes to the geological map of Egypt 1: 500 000 (Conoco Inc., Cairo) 77-140.
3. Soliman S (2013) Mitigation of excessive drawdown via rotational groundwater withdrawal (case study: El Kharga Oasis, Egypt). New York Science J 6: 118-123.
4. Sensoy M, Youssef M, Abdel Zaher M (2013) Sdimentary cover in the South Western Desert of Egypt as deduced from Bouguer gravity and drill-hole data. J of Africa Earth Science 82: 1-14.
5. Hasanien G, Gameh M, Talaat A (2010) Suitability of utilizing shallow groundwater in Kharga Oasis. Assuit Univ Environ Res 13: 27-47.
6. El-Badrawy H, Soliman M (2003) Subsurface evaluation of South Kharga Oasis Area, South Western Desert, Egypt. Egyptian Geophys Soc (EGS) J 1: 31-41.
7. Salman A, Howari F, El-Sankary A, Wali A, Saleh M (2010) Environmental impact and natural hazards on Kharga Oasis monumental sites Western Desert of Egypt. J of Africa Earth Science 58: 341-353.
8. Vozoff k (1991) The magnetotelluric method. In Nabeghian MN (ed) Electromagnetic method in applied geophysics, Society of Exploration Geophysicists, Tusla, Oklahoma 2: 641-711.
9. Metronix Company (2012) Development of broadband magnetotelluric equipment (ADU-7e) and software (Procmt & Maproc), Germany.
10. Constable S, Parker R, deGroot C (1987) Occam's inversion: A practical algorithm for generating smooth models from electromagnetic sounding data. Geophysics 52: 289–300.
11. Siripunvaraporn W, Egbert G, Uyeshima M (2005b) The interpretation of 2-D magnetotelluric profile Data with 3-D Inversion: Synthetic examples. Geophysical J Int 160: 804–814.
12. Mekkawi M, Ogawa Y, Atya M, Ragab E, Arafa-Hamed T, et al. (2014) Magnetotelluric imaging of deep reservoir water in the northern part of Kharga Oasis, Egypt. Proceedings of the Conductivity Anomaly, Titech-Tokyo, Japan.
13. WanNam M, Kim H, Song Y, Lee T, Son J, Suh J (2007) 3D magnetotelluric modeling including surface topography. Geophys Prospect 55: 277-287.
14. Aker P (1991) Advances in three-dimensional magnetotelluric modeling using integral equations. Geophys 56: 1716–1728.
15. Mackie R, Madden T (1993) Three-dimensional magneto telluric inversion using conjugate gradients. Geophys J Int 115: 215–229.
16. Schnegg PA (1999) A computing method for 3D magnetotelluric modelling directed by polynomials. Earth Planets Space 51: 1005–1012.
17. Zhdanov M, Fang S, Hursin G (2000) Electromagnetic inversion using quasi-linear approximation. Geophysics 65: 1501-1513.
18. Sasaki Y (2001) Three-dimensional frequency-domain electromagnetic modelling using the finite-difference method. Butsuri-Tansa 52: 421–432.
19. Muller A, Haak V (2004) 3-D modeling of deep electrical conductivity of Merpi volcano (central Java): Integrating magnetotellurics, induction vectores and the effect of steep topography. J Volcan. Geotherm Res 314-323.
20. Siripunvaraporn W, Egbert G, Lunbury Y, Uyeshima M (2005a) Three-Dimensional Magnetotelluric: data-space method. Physics of the Earth and Planetary Interiors 150: 3–14.
21. Uchida T, Sasaki Y (2006) Stable 3D inversion of MT data and its application to geothermal exploration. Explor Geophys 37: 223-230.
22. Siripunvaraporn W, Egbert G (2009) WSINV3DMT: Vertical magnetic field transfer function inversion and parallel implementation. Physics of the Earth and Planetary Interiors 173: 317–329.
23. Aizawa K, Koyama T, Hase H, Uyeshima M, Kanda W, et al. (2014) Three-dimensional resistivity structure and magma plumbing system of the Kirishima volcanoes as inferred from broad-band magnetotelluric data. J Geophys Res 119: 198–215.
24. Pina-Varas P, Ledo J, Queralt P, Marcuello A, Bellmunt F, et al. (2014) 3-D Magnetotelluric Exploration of Tenerife Geothermal System (Canary Islands, Spain). Surv Geophys 35: 1045-1064.
25. Hersir G, Knútur Arnason, Arnar Mar Vilhjalmsson (2015) 3D inversion of magnetotelluric (MT) resistivity data from Krýsuvík high temperature geothermal area in SW Iceland. Proceedings World Geothermal Congress 2015, Melbourne, Australia 19-25.
26. Egbert G, Kelbert A (2012) Computational recipes for electromagnetic inverse problems. Geophys J Int 189: 251–267.
27. Zhdanov M, Wan L, Gribenko A, Cuma M, Key K, et al. (2011) Large-scale 3D inversion of marine magnetotelluric data: Case study from the Gemini prospect, Gulf of Mexico. Geophysics 76: F77-F87.
28. Patro P, Egbert E (2011) Application of 3D inversion to magnetotelluric profile data from the Deccan Volcanic Province of Western India. Physics of the Earth and Planetary Interiors 187: 33-46.
29. de Groot-Hedlin C, Constable SC (1990) Occam's inversion to generate smooth, two-dimensional models from magnetotelluric data. Geophysics 55: 1613–1624.